Biosensors and Bioelectronics 123 (2019) 152–159

Contents lists available at ScienceDirect

Biosensors and Bioelectronics

journal homepage: www.elsevier.com/locate/bios

Microneedle-based biosensor for minimally-invasive lactate detection

Paolo Bollella[a], Sanjiv Sharma[b], Anthony Edward George Cass[c], Riccarda Antiochia[a,*]

[a] Department of Chemistry and Drug Technologies - Sapienza University of Rome, Rome, Italy
[b] College of Engineering - Swansea University, Swansea, Wales
[c] Department of Chemistry & Institute of Biomedical Engineering - Imperial College, London, UK

ARTICLE INFO

Keywords:
Microneedles
Lactate
Minimally invasive sensors
Continuous monitoring
Interstitial fluid

ABSTRACT

Here we report the first mediated microneedles-based biosensor for minimally invasive continuous sensing of lactate in the dermal interstitial fluid (ISF). To further demonstrate the capability of microneedle arrays as second generation biosensors we have functionalized gold microneedles with nanocarbons at which mediated electron transfer of lactate oxidase takes place. In particular the gold surface of the microneedles electrode has been modified in 3 subsequent steps: i) electrodeposition of Au-multiwalled carbon nanotubes (MWCNTs); ii) electropolymerization of the mediator, methylene blue (MB); iii) immobilization of the enzyme lactate oxidase (LOX) by drop-casting procedure.

The resulting microneedle-based LOX biosensor displays an interference-free lactate detection without compromising its sensitivity, stability, selectivity and response time.

The performance of the microneedle array, second generation biosensor for lactate detection was assessed in artificial interstitial fluid and in human serum, both spiked with lactate. The results reveal that the new microneedles lactate sensor holds interesting promise for the development of a real-time monitoring device to be used in sport medicine and clinical care.

1. Introduction

The real-time monitoring of lactate has attracted great interest in the last few years because it is a key analytical target in sport medicine and clinical care (Gupta et al., 2011; Rassaei et al., 2014). It is known that lactate is an important metabolite formed during the anaerobic metabolism of glucose in muscles. Monitoring of lactate is used to evaluate the maximum performance of an athlete during intensive exercise and endurance-based activities (Gupta et al., 2011, 2013). Lactate concentrations in the blood of healthy individuals ranges from 0.5 to 2 mM at rest rising to 15 mM during exercise and 25 mM under intense physical exercise (Brooks, 1985; Goodwin et al., 2007; Phypers and Pierce, 2006; Stanley et al., 1985). Lactate levels increase also in several pathological conditions, such as cardiac diseases (Karlsson et al., 1975; Valenza et al., 2005) endotoxic shock (Sayeed and Murthy, 1981), pulmonary embolism (De Backer et al., 1997), liver disease (Kruse et al., 1987), diabetes and other disorders (Bellomo, 2002; Rimachi et al., 2012). Lactate has been recently found to be the major cause of acidification in the microenvironment of cancer cells and therefore plays a key role also in cancer diagnosis (Gupta et al., 2015b; Hirschhaeuser et al., 2011).

Blood lactate levels are therefore currently used as an indicator of both fitness and clinical status. There is a great interest in the development of highly sensitive lactate sensors for general clinical diagnostics, intensive care and sport medicine (Srivastava et al., 1995; Vinod, 1995).

Several classical analytical methods have been used, such as amperometry (Nikolaus and Strehlitz, 2008), potentiometry (Shinbo et al., 1979), chemiluminescence (Wu et al., 2005), high-performance liquid chromatography (Omole et al., 1999) and magnetic resonance spectroscopy (Ren et al., 2013). However, these methods have known drawbacks, as they are often time-consuming, expensive and require laboratory equipment and trained personnel (Gupta et al., 2015a, 2012; Srivastava et al., 1996).

Amperometric biosensors represent valid alternatives as they allow accurate and cost-effective determination of lactate in real time with improved sensitivity and selectivity (Dehghani et al., 2016; Gupta et al., 2014a, 2015c; Karimi-Maleh et al., 2015; Karthikeyan et al., 2012).

Numerous amperometric lactate biosensors based on both lactate oxidase (LOX) and lactate dehydrogenase (LDH) immobilized with different strategies on different electrochemical platforms have been previously reported (Agüí et al., 2009; Avramescu et al., 2001; Chen et al., 2017; Collier et al., 1998; Ghamouss et al., 2006; Hickey et al., 2016; Hong et al., 2002; Lamas-Ardisana et al., 2014; Piano et al., 2010;

* Corresponding author.
E-mail address: riccarda.antiochia@uniroma1.it (R. Antiochia).

https://doi.org/10.1016/j.bios.2018.08.010
Received 27 June 2018; Received in revised form 3 August 2018; Accepted 7 August 2018
Available online 10 August 2018
0956-5663/

Rathee et al., 2016; Shimomura et al., 2012). Most of them use blood as the matrix for the analytical detection of lactate with the obvious drawback of having to do repeated finger pricks with the consequent discomfort. Researchers have been recently exhorting the use of minimally invasive sensors to measure lactate concentrations in different biological fluids, such as sweat (Abrar et al., 2016; Anastasova et al., 2017; Jia et al., 2013), saliva (Kim et al., 2014; Petropoulos et al., 2016) and tears (Thomas et al., 2012). Unfortunately, these sensors cannot be as accurate as blood tests because the content of sweat, saliva and tears is more variable as it is can be influenced by other parameters such as the presence of microbes on the skin (in the case of sweat and tears) or by food ingestion (in the case of saliva). The rate of sweating is moreover highly dependent on exercise, temperature and where on the body the measurements are made. Additionally, people aren't always sweating or crying. In many applications outside athletics it is necessary to use wearable bands to locally stimulate sweating.

Microneedle array based biosensors represent an interesting approach as they measure lactate in an under-exploited physiological matrix, the dermal interstitial fluid (ISF), the fluid that bathes the viable tissue of skin (Gupta et al., 2014b; Yola et al., 2014). The interstitial fluid is definitely a more accessible and more reproducible matrix and it seems to be a most suitable human body fluid for the minimally invasive detection of lactate. The ISF microenvironment offer a minimally invasive skin compartment in which to measure biomarkers, many of which show a good correlation with venous blood (Paliwal et al., 2013; Sharma et al., 2017). Due to the small dimensions of the microneedles (1 mm length), they can penetrate the stratum corneum but they do not reach deep into the sub-cutaneous tissue, unlike the needle sensors used, for example, in commercially available continuous glucose monitoring (CGM) devices. Measurements are made in the upper part of dermal interstitial compartment where no blood vessels and no nerve endings are present (Sharma et al., 2017), as shown in Fig. 1B. For these reasons, compared to other continuous monitoring devices, the microneedle arrays offer the following advantages: i) minimal invasiveness, thanks to their small dimensions; ii) reduced biofouling effects, as they are changed on a daily basis (24–48 h maximum) while the other devices are implanted for 7–14 days; iii) larger currents because of their larger electrode surface areas. Moreover, the minimally invasive nature of the microneedle arrays suggests that they are associated with less skin irritation, reduced pain and tissue trauma, lower risk of local infection and lower risk of bleeding. A full recovery is observed within 24 h of removal (El-Laboudi et al., 2013) and often less.

Furthermore, a wide range of vital information can be obtained from skin interstitial fluid (ISF) in a completely non-invasive and continuous fashion. Over the past three decades, researchers have used the ISF for non-invasive detection of inherited metabolic diseases, organ failure, and drug efficacy (El-Laboudi et al., 2013; Windmiller et al., 2011). Most of the attention has been devoted on glucose monitoring in ISF (Miller et al., 2016; Sharma et al., 2016; Valdés-Ramírez et al., 2014; Ventrelli et al., 2015). the correlation between ISF and blood lactate has prompted several industrial and academic researchers to develop optical-, ultrasound-, heat-, and electrochemical-based devices for continuous, non-invasive lactate monitoring (Abrar et al., 2016; Miller et al., 2012; Sharma et al., 2017). Besides the aforementioned analytes, also alcohol has been detected in ISF (Mohan et al., 2017).

The present work describes the first example of a mediated pain free microneedle-based biosensor for the continuous monitoring of lactate in the ISF. The gold surface of the microneedles has been modified by electrodeposition of Au-multiwalled carbon nanotubes (MWCNTs) and successively by electropolymerization of the redox mediator, methylene

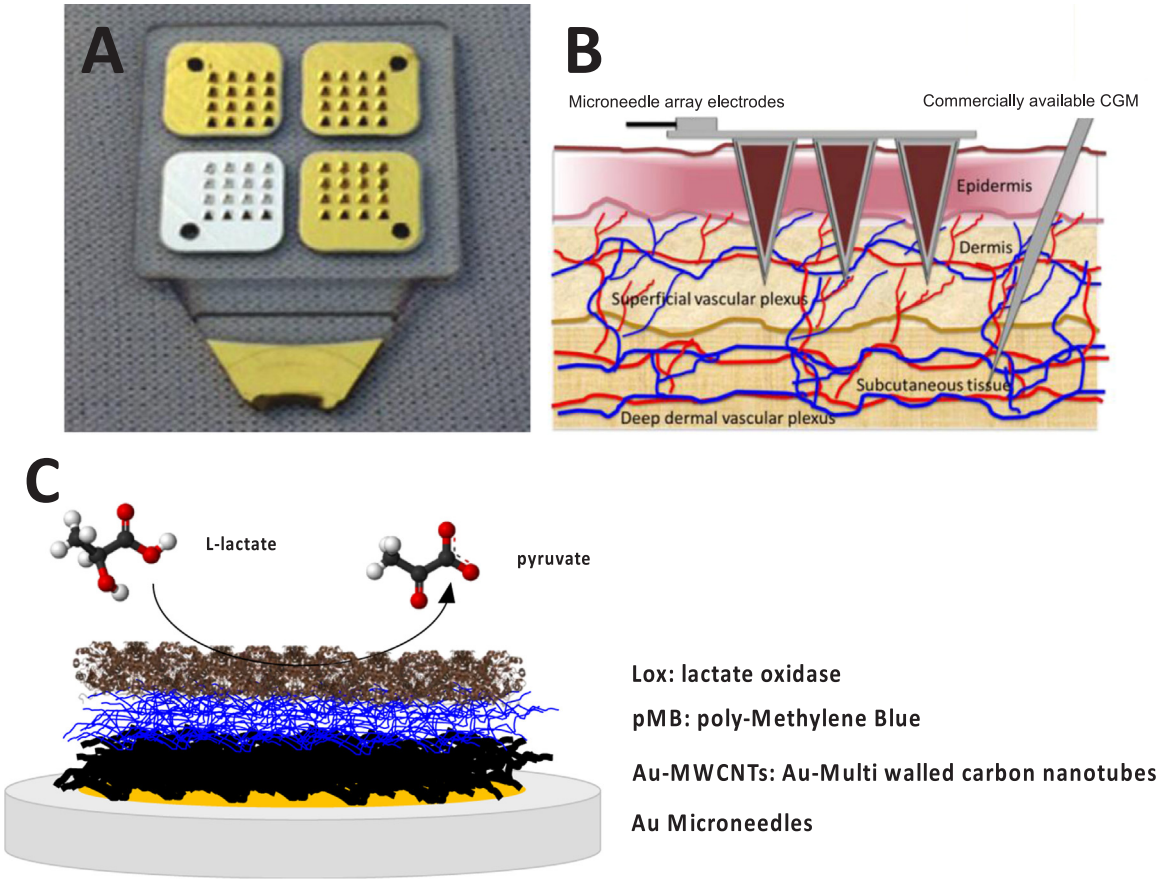

Fig. 1. (A) Polycarbonate structure of four 4 × 4 microneedle arrays metallized with gold and silver; (B) Sketch of the outermost layers of the human skin, epidermis and dermis and of the two different approaches used (microneedles arrays and commercial CGM devices) to access the interstitial fluid; (C) Schematic representation of the modified electrode. Figs. A and B are reproduced from Sharma et al. (2016) with permission of Springer Berlin Heidelberg.

blue (MB). Functionalization of the Au-MWCNTs/polyMB platform with the LOX enzyme by drop casting procedure enabled the continuous monitoring of lactate in artificial interstitial fluid and in human serum.

The interesting analytical performances exhibited by the new microneedles based biosensor makes it a promising tool as a minimally invasive wearable monitoring device for continuous monitoring of lactate to be used in sport medicine and clinical care.

2. Experimental

2.1. Chemicals and reagents

3-(N-morpholino)propanesulfonic acid (MOPS), 4-(2-Hydroxyethyl) piperazine-1-ethanesulfonic acid (HEPES), ammonium chloride (NH_4Cl), ascorbic acid (AA), boric acid, calcium chloride ($CaCl_2$), D-(-)-glucose (Glc), ferricynide ($Fe(CN)_6^{3-}$), ferrocyanide ($Fe(CN)_6^{4-}$), human serum from human male AB plasma (USA origin, sterile-filtered), magnesium sulfate ($MgSO_4$), methylene blue (MB), multi-walled carbon nanotubes (MWCNTs), potassium chloride (KCl), potassium nitrate (KNO_3), saccharose, sodium acetate (CH_3COONa), sodium tetraborate, sodium chloride (NaCl) sodium L-lactate, sodium phosphate dibasic (Na_2HPO_4), sodium phosphate monobasic (NaH_2PO_4), sulfuric acid (H_2SO_4), tris(hydroxymethyl)aminomethane (TRIS) and uric acid (UA) were obtained from Sigma Aldrich (St. Louis, MO, USA).

Lactate oxidase (LOX) from *Aerococcus Viridans* (Umena et al., 2006) was obtained from Creative Enzyme Ltd. The LOX (activity 106 U/mL) was dissolved in a phosphate buffer at pH 6.5, divided into aliquots, and kept at −20 °C until immediately before being used.

All solutions were prepared using Milli-Q water (18.2 MΩ cm, Millipore, Bedford, MA, USA).

2.2. Electrode preparation and modification

2.2.1. Gold planar electrodes

Polycrystalline gold electrodes (AuE) (d = 2 mm, AMEL, Milano, ITALY) were cleaned by incubation in Piranha solution for 2 min (1:3 mixture of conc. H_2O_2 (30%) with H_2SO_4, *CAUTION: Piranha solution is especially dangerous, corrosive and may explode if contained in a closed vessel, it should be handled with special care*), then with polishing cloths with deagglomerated alumina slurry of 1 μm diameter (SIEM, Bologna, ITALY), successively sonicated in ultrapure water for 5 min and finally electrochemically cleaned in 0.5 M H_2SO_4 by cycling 20 times between − 0.3 and 1.7 V vs. SCE at a scan rate of 300 mV s^{-1}. Polycrystalline gold electrodes were modified by electrodeposition of Au-MWCNTs sweeping the potential between 0.8 and 0 V vs. SCE for 25 scans at 50 mV s^{-1} in a suspension containing 5 mg/mL of MWCNTs (10 mM $HAuCl_4$ in 2.5 M NH_4Cl) (Dai and Compton, 2006). The modified electrodes were characterized in 5 mM $Fe(CN)_6^{3-/4-}$ (50 mM PBS buffer pH 7.4 + 137 mM NaCl) in order to determine the electroactive surface area, heterogeneous electron transfer rate constant (k°, cm s^{-1}) and roughness factor (ρ). Afterwards, the so prepared AuE/Au-MWCNTs were further modified by electrodeposition of pMB sweeping the potential between −0.4 and 1.2 vs. SCE in 0.25 mM MB solution (0.02 M borate buffer pH 9.14, supporting electrolyte 0.1 M KNO_3, sweep rate 50 mV s^{-1}) (Karyakin et al., 1999). Next, 5 μL of LOX were drop-cast onto the modified electrode and left to dry at room temperature. Finally, the electrode was gently rinsed with 50 mM PBS buffer (pH 7.4) and stored at 4 °C overnight.

2.2.2. Au microneedles electrodes

The microneedle array base structures were fabricated in polycarbonate at Glasgow University, as described in detail previously (Cass and Sharma, 2017) and metallized by Torr Scientific Ltd (Bexhill). They consist of a polycarbonate structure (1.0 × 1.0 × 0.2 cm) consisting of 64 microneedles perpendicular to the base plate arranged as four 4 × 4 arrays (pyramid dimensions: base 0.06 cm, height 0.1 cm; 4 × 4 array area: 0.2 cm^2), as shown in Fig. 1A. Three of them have been metallized with gold and are used as working electrodes and one has been metallized with silver. However in this work, in vitro, an external saturated calomel electrode was used as the reference electrode.

The microneedle electrodes were electrochemically cleaned in 0.5 M H_2SO_4 by cycling 20 times between −0.3 and 1.7 V vs. SCE at a scan rate of 300 mV s^{-1} and successively modified by electrodeposition of Au-MWCNTs, characterized in 5 mM $Fe(CN)_6^{3-/4-}$ in order to determine the electroactive surface area, heterogeneous electron transfer rate constant (k°, cm s^{-1}) and roughness factor (ρ) and finally modified by electrodeposition of pMB and by drop casting of LOX, according to the same procedures as reported for the gold planar electrodes (paragraph 2.2.1).

2.3. SEM experiments

Scanning electron microscopy (SEM) measurements were performed with High-Resolution Field Emission Scanning Electron Microscopy (HR FESEM, Zeiss Auriga Microscopy, Jena, Germany). All samples were prepared according to the modification protocol, as reported in Section 2.2, using gold plates (25 Å∼ 25 Å∼ 1 mm, ALS Co. Ltd., Tokyo, Japan) instead of gold electrodes and Au microneedles electrodes.

2.4. Preparation of artificial interstitial fluid

The artificial interstitial fluid (ISF) was prepared by mixing 2.5 mM $CaCl_2$, 5.5 mM glucose, 10 mM Hepes, 3.5 mM KCl, 0.7 mM $MgSO_4$, 123 mM NaCl, 1.5 mM NaH_2PO_4, 7.4 mM saccharose. The pH was adjusted to pH 7.4 (Saito et al., 2017).

2.5. Electrochemical measurements

Cyclic voltammetry and amperometric experiments were performed by using a PGSAT204N potentiostat (Eco Chemie, The Netherlands) controlled by Nova 2.1 software (Eco Chemie, The Netherlands) with a conventional three-electrodes electrochemical cell equipped with a modified gold planar electrode or Au microneedles as working electrodes, a saturated calomel electrode (SCE, 244 mV vs. NHE, Cat. 303/SCG/12, AMEL, Milano, Italy) and a glassy carbon rod electrode (d = 2 mm, Cat. 6.1241.020, Metrohm, Herisau, Switzerland) were used as reference and counter electrodes, respectively. The temperature-controlled experiments were carried out by using a thermostatic bath (T ± 0.01 °C, LAUDA RM6, Delran, NJ, USA).

3. Results and discussion

3.1. Microneedles surface functionalization

The working gold surface of the microneedles has been functionalized initially by electrodeposition of Au-multiwalled carbon nanotubes (MWCNTs), followed by electropolymerization of methylene blue (MB) and finally by immobilization of the enzyme lactate oxidase (LOX) by drop-casting procedure (Fig. 1C).

SEM images were used to evaluate the physical appearance and the surface characteristics of the gold microneedles electrode before and after the electrodeposition of Au-MWCNTs, obtained by cycling the potential between 0.8 and 0 V for 25 cycles. Fig. 2 shows the SEM images relative to the bare gold microneedles electrode (Fig. 2A) and to the Au-MWCNTs microneedles electrode at two different magnifications (Fig. 2B and C). The optimal surface coverage obtained is probably due to the initial reduction of Au^{3+} to Au° with the formation of Au nanoparticles onto the electrode surface which allow the entrapment of the MWCNTs. This process is further facilitated by the formation of stacking interactions between the nanotubes allowing a good coating. The unmodified and the Au-MWCNTs modified microneedles electrodes were successively characterized by cyclic voltammetry experiments in a

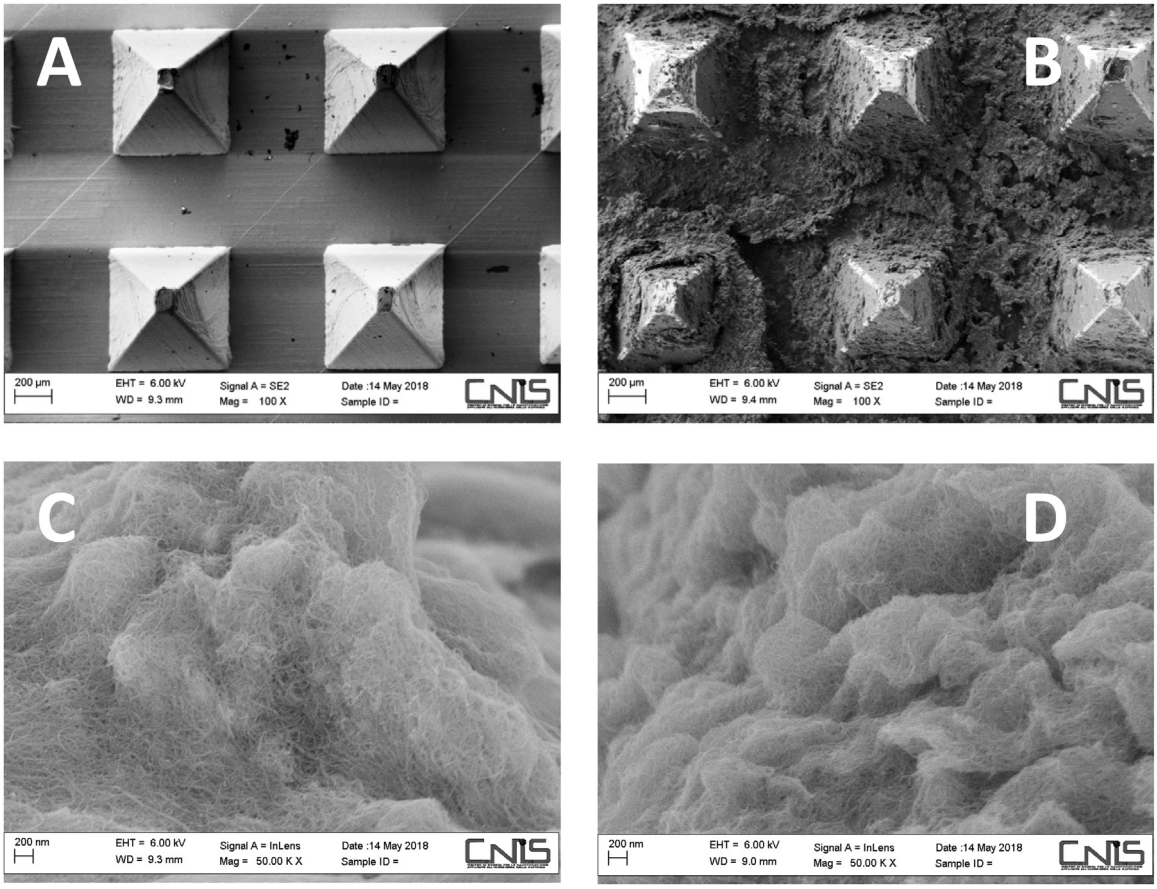

Fig. 2. SEM images of: bare Au microneedle electrode (A); Au microneedle/Au-MWCNTs electrode at two different magnifications (B, C); Au microneedle/Au-MWCNTs/pMB electrode (D).

solution of $Fe(CN)6^{3-}/^{4-}$ (Fig. 1S). The CVs shows the faradaic peak for the oxidation of Fe^{2+} to Fe^{3+} in the forward scan and also the faradaic peak for the reduction process in the reverse scan. Although there is no great difference in terms of potential difference between the anodic and the cathodic peak ($\Delta E_p = E_a\text{-}E_c$) at 50 mV s^{-1} (Au and Au/Au-MWCNTs ΔE_p = 78 mV, Au microneedles and Au microneedles/Au-MWCNTs ΔE_p =63 mV), it is possible to note the large enhance of the anodic and cathodic peak current densities after the Au-MWCNTs electrodeposition due to the increase of the electroactive surface area. It is interesting to observe that this effect is much more evident in the case of the microneedles electrode (Fig. 1S B) compared to the planar gold electrode (Fig. 1S A), as confirmed by the roughness factor which resulted to be almost ten times higher in the case of the microneedles electrode (ρ = 301.6 ± 1.6) compared to the planar electrode (ρ = 39.5 ± 0.6). This result can be ascribed to the fact that the particular geometry of the microneedles might allow a better electrodeposition of the MWCNTs and therefore a larger electroactive surface area. The heterogeneous electron transfer rate constants (k°, cm s^{-1}) have also been calculated using the extended method which merges the Klingler-Kochi and Nicholson and Shain methods for totally irreversible and reversible systems (Lavagnini et al., 2004, 2007). The k_0 value obtained in the case of the Au microneedles/Au-MWCNTs electrode resulted to be much higher (k_0 = 16.3 ± 0.4 × 10^3 cm s^{-1}) than that obtained in the case of the planar Au electrode modified with Au-MWCNTs (k_0 = 2.7 ± 0.9 × 10^3 cm s^{-1}), showing a faster electron transfer kinetics.

The Au-MWCNTs microneedles electrode was successively modified by electrodeposition of the redox mediator methylene blue, by cycling the potential values from −0.4 to 1.2 V vs. SCE for 25 cycles in borate buffer pH 9.1. Fig. 2D show the SEM image of the Au microneedle/Au-MWCNTs/polyMB modified electrode. The voltammetric profile of the formation of the polymeric film shows two couples of redox peaks (Fig. 2S). As the electropolymerization process takes place, the couple of peaks which appears at more negative potentials decreases and a new set of peaks appears at more positive potentials. This response is typical of a polymer-type redox activity, which is usually shifted to more positive potentials compared to the monomer (Karyakin et al., 1999). The cyclic voltammogram of the Au-MWCNTs/polyMB modified microneedle electrode is shown in Fig. 3S. Two pairs of quasi-reversible redox peaks are clearly visible in the voltammogram. The first one corresponds to the monomer, the additional one to the polyMB and is located at a 200 mV more anodic potential, according to data reported in literature for electropolymerized amines (Braun et al., 2017; Liu and Mu, 1999).

3.2. Electrochemical characterization of lactate sensor

Lactate biosensors were prepared by drop-casting LOX enzyme onto the Au-MWCNTs/pMB microneedle electrode surface. In order to optimize the enzyme concentration, different biosensors were prepared by drop-casting different LOX amounts on the microneedles surface. The effect of enzyme loading on the current response was investigated in the range from 1U to 5 U of LOX. The current density increased when the concentration of LOX increased from 1 to 1.5 U showing a slight decrease at higher enzyme concentrations (Fig. 4S A). The amount of enzyme is therefore rate limiting at low enzyme amounts loaded but at higher concentrations the reaction becomes limited by other factors. A concentration of 1.5 U was chosen for further experiments. The biosensor performance was also tested by varying the concentration of MWCNTs used during the electrodeposition process and the electrodeposition number cycles (Fig. 4S B and C). The results confirmed that

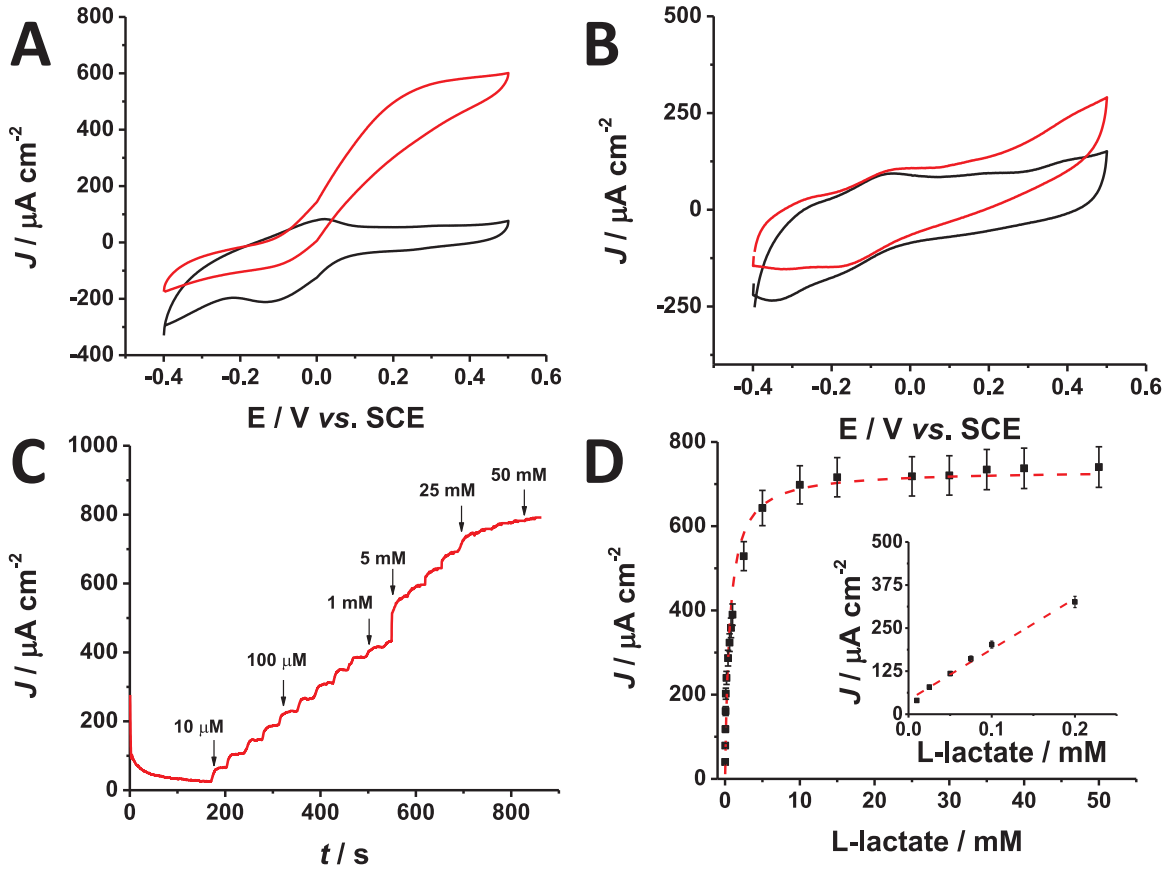

Fig. 3. Cyclic voltammograms of Au microneedle/Au-MWCNTs/pMB/LOX (A) and Au bare/Au-MWCNTs/pMB/LOX in absence (black) and in presence (red) of 10 mM sodium L-lactate in 50 mM PBS buffer pH 7.4 with 137 mM NaCl at ν = 5 mV s^{-1}. (C) Chronoamperometric response of Au microneedles/Au-MWCNTs/pMB/LOX in 50 mM PBS buffer with 137 mM NaCl. (D) Calibration curve of the Au microneedles/Au-MWCNTs/pMB/LOX based biosensor in 50 mM PBS buffer with 137 mM NaCl. Inset: low micromolar range. Experimental conditions: applied potential + 0.15 V vs. SCE, adding time = 40 s, under stirring = 400 rpm and T = 25 °C.

the highest current signal was obtained by cycling the potential for 25 cycles in a solution of 5 mg/mL MWCNTs, conditions used for the microneedle surface functionalization experiments.

A comparative cyclic voltammogram of the Au-MWCNTs/pMB/LOX microneedle electrode in the absence and in the presence of lactate is shown in Fig. 3 A. The black curve shows no significant difference with the CV of the modified electrode without enzyme (curve not shown), thus indicating that no significant change has been observed after the immobilization of LOX. It is possible to note a very good electrocatalytic current with an onset potential of −90 mV, close to the redox potential of the mediator pMB (E_0 = -95 mV vs. SCE). Such low potential for lactate oxidation reflects the efficient electron donor-acceptor interactions between the carbon nanotubes and the mediator, which supports the shuttling of the electrons between the redox center of the enzyme and the electrode surface. A potential of + 0.15 V vs SCE reference electrode was thus selected for further experiments. If we compare these results with those obtained with a planar gold electrode modified exactly in the same way, we can see that the electrocatalytic current obtained with the microneedles is almost three times higher than that obtained with the planar electrode (Fig. 3 B). This result can be explained by the fact that the geometry of the microneedle electrodes might enable faster diffusion of the substrate to the electrode surface (Belding et al., 2010; Menshykau et al., 2008).

The analytical response of the microneedle biosensor towards lactate was evaluated by chronoamperometry (Fig. 3 C). The calibration curve for lactate detection, shown in Fig. 3 D, indicates a linear range from 10 µM to 200 µM lactate, a detection limit of 2.4 µM (based on S/N = 3) and a very high sensitivity of 1473 µA cm^{-2} mM^{-1} and a correlation coefficient of 0.98 (RSD 5.0%, n = 3). Additionally, the calibration curve was fitted to the classical Michaelis-Menten kinetic parameters, which resulted in a J_{max} of 733 ± 19 µA cm^{-2} and an apparent Michaelis-Menten constant (K_M) of 0.64 ± 0.1 mM.

3.3. Effect of pH and temperature on biosensor response

The effects of pH and temperature on the proposed lactate biosensor were evaluated and the results are shown in Fig. 4 A and B. Four different buffers have been tested, acetate, MOPS, phosphate and TRIS buffer in order to cover the range of pHs between 2 and 9. The current signal increased with pH until a pH value of 7.5, which corresponds to the maximum current signal obtained in both phosphate buffer and TRIS buffer (Fig. 4A). A pH 7.5 in phosphate buffer is therefore chosen for our experiments because phosphate buffer is the closest to physiological conditions. The optimum temperature resulted to be 35 °C, as shown in Fig. 4B. These results are in close agreement with the optimum pH and T values reported in literature for lactate oxidase (Taurino et al., 2016).

3.4. Study of biosensor stability

The stability and lifetime of the biosensor were investigated by monitoring the signal decrease of the current when the biosensor is used for 20 measurements every day over a period of 30 days for a 0.2 mM lactate solution, as reported in Fig. 4C. The microneedles based biosensor showed a signal decrease of its initial response of less than 10% after 30 days, probably due to a combination of the intrinsic stability of the enzyme, the nanostructuring of the microneedle electrode surface and to the particular geometry of the microneedles themselves.

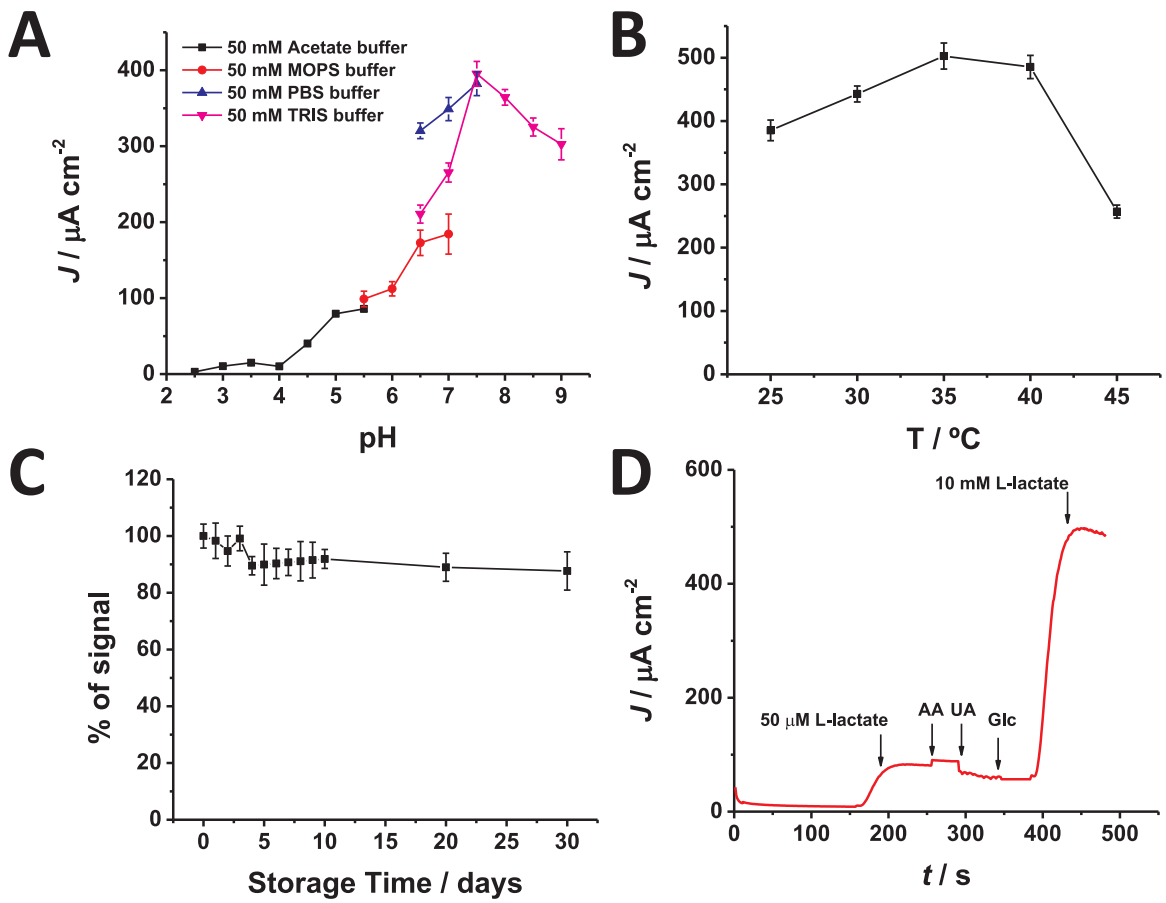

Fig. 4. Effect of different pHs (A) and temperature (B) on Au microneedle/Au-MWCNTs/pMB/LOX based biosensor: 50 mM acetate buffer (black), 50 mM MOPS buffer; 0.2 mM L-lactate (red), 50 mM phosphate buffer (blue) and TRIS buffer (pink). Experimental conditions: 0.2 mM L-lactate, applied potential + 0.15 V. (C) Stability measurements carried out over a period of 30 days in presence of 0.2 mM L-lactate in 50 mM TRIS buffer; E_{app} = 0.150 vs. SCE; T = 25 °. (D) Influence of interfering compounds on lactate response: 50 µM L-lactate, 50 µM ascorbic acid (AA), 50 µM uric acid (UA), 50 µM glucose (Glc) and 10 mM L-lactate. Experimental conditions: applied potential + 0.15 V vs. SCE, adding time = 40 s, under stirring = 400 rpm and T = 25 °C.

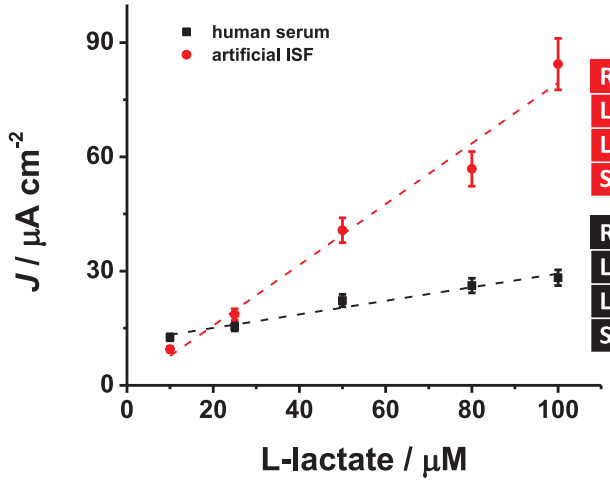

R^2	0.96
LOD / µM	3
Linear range / µM	10-100
Sensitivity / µA cm^{-2} mM^{-1}	797.4 ± 38.1

R^2	0.98
LOD / µM	3.2
Linear range / µM	10-100
Sensitivity / µA cm^{-2} mM^{-1}	178.4 ± 9.2

Fig. 5. Calibration curves of the Au microneedles/Au-MWCNTs/pMB/LOX based lactate biosensor in artificial interstitial fluid (red curve) and in human serum (black curve), both spiked with lactate. Experimental conditions: applied potential + 0.15 V vs. SCE, adding time = 40 s, under stirring = 400 rpm and T = 25 °C.

3.5. Interference study

The selectivity of the biosensor was studied in order to assess the influence of possible interfering compounds on its response. The signal obtained for a fixed concentration of lactate was compared to that obtained with equal amounts of interfering compounds such as ascorbic acid, uric acid and glucose. The differences in peak current were all less than 5% in the presence of ascorbic acid and less than 1% in the presence of uric acid and glucose (Fig. 4D). Such high selectivity reflects the low operating potential of the second generation biosensor, due to

Table 1
Comparison with other non invasive amperometric lactate biosensors reported in literature.

Electrode Material	Sensing Fluid	Sensor type	Linear range (mM)	Sensitivity	Enzyme	Generation	References
AgNPs	sweat	bendable	1–25	0.26 μA mM^{-1} cm^{-2}	*Pediococcus* sp.	1st	Abrar et al. (2016)
CNTs-Ag/AgCl	sweat	bendable	1–20	10.31 μA μM^{-1} cm^{-2}	*microorganism*	2nd	Wang et al. 2013
Gr + PB, Ag/AgCl integrated in a mouthguard	saliva	printable on curved surface	0.1–1	0.55 μA mM^{-1}	*microrganism*	1st	Wang et l. 2014
Ti/Pd/Pt integrated in contact lens	tears	rigid type film	0–1	53 μA mM^{-1} cm^{-2}	*Aerococcus viridans*	1st	Thomas et al. (2012)
Au microneedles/Au-MWCNTs/pMB	interstitial fluids	bendable	0.01–0.2	1473 μA mM^{-1} cm^{-2}	*Aerococcus viridans*	2nd	This Work

the combined use of the electropolymerized MB and a nanostructured surface.

3.6. Analysis of artificial interstitial fluid and human serum

In order to demonstrate the feasibility of the modified microneedles based electrode for the minimally invasive detection of lactate, the biosensor was used to determine the concentration of lactate in artificial interstitial fluid and human blood samples, both spiked with lactate. Fig. 5 shows the calibration plots obtained with artificial ISF and human serum. The response is linear in both case with a similar detection limit, but a narrower linear range compared to that reported previously in phosphate buffer pH 7.5. The sensitivities resulted to be 800 ± 38 μA cm^{-2} mM^{-1} in ISF (RSD 4.8%, n = 3) and 180 ± 9 μA cm^{-2} mM^{-1} (RSD 5.2%, n = 3) in human serum, lower than that obtained in phosphate buffer. This result is particularly evident with the measurements carried out in human serum where the measurements may be affected by biofouling effects of the electrode. However, the response obtained in the ISF remains high enough to allow a good detection of lactate and indicates the potential for the subcutaneous lactate monitoring based on the proposed microneedles based biosensor.

Table 1 shows a comparison of the results obtained with other non-invasive amperometric lactate biosensors reported in literature. Lactate was detected in different biological fluids such as sweat, saliva and tears. As we can see, the linear range is broader but the sensitivity obtained is definitely lower than that obtained with the microneedles-based biosensor.

It is important to note that the content of sweat, saliva and tears is more variable compared to the composition of blood and of interstitial fluid. It can be influenced by different factors such as microbes on the skin (in the case of sweat and tears) or by food ingestion (in the case of saliva). Moreover, as people aren't always sweating, in many applications outside athletics it is necessary to use wearable bands to locally stimulate sweating. The interstitial fluid is an accessible and more reproducible matrix and it seems to be the most suitable human body fluid for the minimally invasive measurement of lactose.

4. Conclusions

This study has demonstrated the design and development of the first example of a second generation minimally invasive biosensor for lactate detection based on microneedle arrays. The new biosensor device is based on the use of a gold microneedles electrode modified with MWCNTs, polymethylene blue and lactate oxidase from *Aereococcus viridans*. The system enables highly sensitive, selective and stable determination of lactate in human interstitial fluid, which suggests that it is a suitable body fluid compared to sweat, saliva and tears, as it is expected to show less variability in its composition. For these reasons the lactate biosensor based on microneedle technology seems to be a promising tool as a wearable device to be used in sport medicine and in clinical care for continuous monitoring of lactate. The biosensor will be further optimized and validated for in vivo measurements through clinical studies with healthy volunteers.

Future efforts will focus on integration of the instrumentation for signal processing and wireless communication, as well as on a critical evaluation of the tolerability and biocompatibility of the device.

Acknowledgements

The authors would like to thank the Italian Research Council for financial support. The authors would like to acknowledge Dr. Francesco Mura to help in SEM pictures handling of modified electrodes (CNIS, Sapienza University of Rome).

Appendix A. Supporting information

Supplementary data associated with this article can be found in the online version at doi:10.1016/j.bios.2018.08.010.

References

Abrar, M.A., Dong, Y., Lee, P.K., Kim, W.S., 2016. Bendable electro-chemical lactate sensor printed with silver nano-particles. Sci. Rep. 6, 30565.
Agüí, L., Eguilaz, M., Peña-Farfal, C., Yáñez-Sedeño, P., Pingarron, Je.M., 2009. Lactate dehydrogenase biosensor based on an hybrid carbon nanotube-conducting polymer modified electrode. Electroanalysis 21 (3-5), 386–391.
Anastasova, S., Crewther, B., Bembnowicz, P., Curto, V., Ip, H.M., Rosa, B., Yang, G.-Z., 2017. A wearable multisensing patch for continuous sweat monitoring. Biosens. Bioelectron. 93, 139–145.
Avramescu, A., Noguer, T., Magearu, V., Marty, J.-L., 2001. Chronoamperometric determination of D-lactate using screen-printed enzyme electrodes. Anal. Chim. Acta 433 (1), 81–88.
Belding, S.R., Campbell, F.W., Dickinson, E.J., Compton, R.G., 2010. Nanoparticle-modified electrodes. Phys. Chem. Chem. Phys. 12 (37), 1208–11221 (1).
Bellomo, R., 2002. Bench-to-bedside review: lactate and the kidney. Crit. Care 6 (4), 322–326.
Braun, W.A., Horn, B.C., Hoehne, L., Stülp, S., Rosa, M.B., Hilgemann, M., 2017. Poly (methylene blue)-modified electrode for indirect electrochemical sensing of OH radicals and radical scavengers. An. Acad. Bras. Ciências 89 (3), 1381–1389.
Brooks, G.A., 1985. Anaerobic threshold: review of the concept and directions for future research. Med. Sci. Sports Exerc. 17 (1), 22–34.
Cass, A.E., Sharma, S., 2017. Microneedle enzyme sensor arrays for continuous in vivo monitoring. In: Methods in Enzymology. Elsevier, pp. 413–427.
Chen, Q., Sun, T., Song, X., Ran, Q., Yu, C., Yang, J., Feng, H., Yu, L., Wei, D., 2017. Flexible electrochemical biosensors based on graphene nanowalls for the real-time measurement of lactate. Nanotechnology 28 (31), 315501.
Collier, W., Lovejoy, P., Hart, A., 1998. Estimation of soluble L-lactate in dairy products using screen-printed sensors in a flow injection analyser. Biosens. Bioelectron. 13 (2), 219–225.
Dai, X., Compton, R.G., 2006. Direct electrodeposition of gold nanoparticles onto indium tin oxide film coated glass: application to the detection of arsenic (III). Anal. Sci. 22 (4), 567–570.
De Backer, D., Creteur, J., Zhang, H., Norrenberg, M., Vincent, J.-L., 1997. Lactate production by the lungs in acute lung injury. Am. J. Respir. Crit. Care Med. 156 (4), 1099–1104.
Dehghani, M.H., Sanaei, D., Ali, I., Bhatnagar, A., 2016. Removal of chromium (VI) from aqueous solution using treated waste newspaper as a low-cost adsorbent: kinetic modeling and isotherm studies. J. Mol. Liq. 215, 671–679.
El-Laboudi, A., Oliver, N.S., Cass, A., Johnston, D., 2013. Use of microneedle array devices for continuous glucose monitoring: a review. Diabetes Technol. Ther. 15 (1),

101–115.
Ghamouss, F., Ledru, S., Ruillé, N., Lantier, F., Boujtita, M., 2006. Bulk-modified modified screen-printing carbon electrodes with both lactate oxidase (LOD) and horseradish peroxide (HRP) for the determination of L-lactate in flow injection analysis mode. Anal. Chim. Acta 570 (2), 158–164.
Goodwin, M.L., Harris, J.E., Hernández, A., Gladden, L.B., 2007. Blood lactate measurements and analysis during exercise: a guide for clinicians. J. Diabetes Sci. Technol. 1 (4), 558–569.
Gupta, V.K., Ganjali, M., Norouzi, P., Khani, H., Nayak, A., Agarwal, S., 2011. Electrochemical analysis of some toxic metals by ion–selective electrodes. Crit. Rev. Anal. Chem. 41 (4), 282–313.
Gupta, V.K., Karimi-Maleh, H., Sadegh, R., 2015a. Simultaneous determination of hydroxylamine, phenol and sulfite in water and waste water samples using a voltammetric nanosensor. Int. J. Electrochem. Sci. 10, 303–316.
Gupta, V.K., Kumar, S., Singh, R., Singh, L., Shoora, S., Sethi, B., 2014a. Cadmium (II) ion sensing through p-tert-butyl calix [6] arene based potentiometric sensor. J. Mol. Liq. 195, 65–68.
Gupta, V.K., Mergu, N., Kumawat, L.K., Singh, A.K., 2015b. A reversible fluorescence "off–on–off" sensor for sequential detection of aluminum and acetate/fluoride ions. Talanta 144, 80–89.
Gupta, V.K., Mergu, N., Kumawat, L.K., Singh, A.K., 2015c. Selective naked-eye detection of magnesium (II) ions using a coumarin-derived fluorescent probe. Sens. Actuators B: Chem. 207, 216–223.
Gupta, V.K., Sethi, B., Sharma, R., Agarwal, S., Bharti, A., 2013. Mercury selective potentiometric sensor based on low rim functionalized thiacalix [4]-arene as a cationic receptor. J. Mol. Liq. 177, 114–118.
Gupta, V.K., Singh, A.K., Kumawat, L.K., 2014b. Thiazole Schiff base turn-on fluorescent chemosensor for Al3+ ion. Sens. Actuators B: Chem. 195, 98–108.
Gupta, V.K., Singh, L., Singh, R., Upadhyay, N., Kaur, S., Sethi, B., 2012. A novel copper (II) selective sensor based on dimethyl 4, 4′(o-phenylene) bis (3-thioallophanate) in PVC matrix. J. Mol. Liq. 174, 11–16.
Hickey, D.P., Reid, R.C., Milton, R.D., Minteer, S.D., 2016. A self-powered amperometric lactate biosensor based on lactate oxidase immobilized in dimethylferrocene-modified LPEI. Biosens. Bioelectron. 77, 26–31.
Hirschhaeuser, F., Sattler, U.G., Mueller-Klieser, W., 2011. Lactate: a metabolic key player in cancer. Cancer Res. 71 (22), 6921–6925.
Hong, M.-Y., Chang, J.-Y., Yoon, H.C., Kim, H.-S., 2002. Development of a screen-printed amperometric biosensor for the determination of L-lactate dehydrogenase level. Biosens. Bioelectron. 17 (1–2), 13–18.
Jia, W., Bandodkar, A.J., Valdés-Ramírez, G., Windmiller, J.R., Yang, Z., Ramírez, J., Chan, G., Wang, J., 2013. Electrochemical tattoo biosensors for real-time noninvasive lactate monitoring in human perspiration. Anal. Chem. 85 (14), 6553–6560.
K Gupta, V., Nayak, A., Agarwal, S., Singhal, B., 2011. Recent advances on potentiometric membrane sensors for pharmaceutical analysis. Comb. Chem. High Throughput Screen. 14 (4), 284–302.
Karimi-Maleh, H., Tahernejad-Javazmi, F., Atar, N., Yola, M.Lt, Gupta, V.K., Ensafi, A.A., 2015. A novel DNA biosensor based on a pencil graphite electrode modified with polypyrrole/functionalized multiwalled carbon nanotubes for determination of 6-mercaptopurine anticancer drug. Ind. Eng. Chem. Res. 54 (14), 3634–3639.
Karlsson, J., Willerson, J., Leshin, S., Mullins, C., Mitchell, J., 1975. Clinical physiology: skeletal muscle metabolites in patients with cardiogenic shock or severe congestive heart failure. Scand. J. Clin. Lab. Investig. 35 (1), 73–79.
Karthikeyan, S., Gupta, V., Boopathy, R., Titus, A., Sekaran, G., 2012. A new approach for the degradation of high concentration of aromatic amine by heterocatalytic Fenton oxidation: kinetic and spectroscopic studies. J. Mol. Liq. 173, 153–163.
Karyakin, A.A., Karyakina, E.E., Schmidt, H.L., 1999. Electropolymerized azines: a new group of electroactive polymers. Electroanal.: Int. J. Devoted Fundam. Pract. Asp. Electroanal. 11 (3), 149–155.
Kim, J., Valdés-Ramírez, G., Bandodkar, A.J., Jia, W., Martinez, A.G., Ramírez, J., Mercier, P., Wang, J., 2014. Non-invasive mouthguard biosensor for continuous salivary monitoring of metabolites. Analyst 139 (7), 1632–1636.
Kruse, J.A., Zaidi, S.A., Carlson, R.W., 1987. Significance of blood lactate levels in critically III patients with liver disease. Am. J. Med. 83 (1), 77–82.
Lamas-Ardisana, P.J., Loaiza, O.A., Añorga, L., Jubete, E., Borghei, M., Ruiz, V., Ochoteco, E., Cabañero, G., Grande, H.J., 2014. Disposable amperometric biosensor based on lactate oxidase immobilised on platinum nanoparticle-decorated carbon nanofiber and poly (diallyldimethylammonium chloride) films. Biosens. Bioelectron. 56, 345–351.
Lavagnini, I., Antiochia, R., Magno, F., 2004. An extended method for the practical evaluation of the standard rate constant from cyclic voltammetric data. Electroanalysis 16 (6), 505–506.
Lavagnini, I., Antiochia, R., Magno, F., 2007. A calibration-base method for the evaluation of the detection limit of an electrochemical biosensor. Electroanalysis 19 (11), 1227–1230.
Liu, J., Mu, S., 1999. The electrochemical polymerization of methylene blue and properties of polymethylene blue. Synth. Metals 107 (3), 159–165.
Menshykau, D., Streeter, I., Compton, R.G., 2008. Influence of electrode roughness on cyclic voltammetry. J. Phys. Chem. C 112 (37), 14428–14438.
Miller, P.R., Narayan, R.J., Polsky, R., 2016. Microneedle-based sensors for medical diagnosis. J. Mater. Chem. B 4 (8), 1379–1383.
Miller, P.R., Skoog, S.A., Edwards, T.L., Lopez, D.M., Wheeler, D.R., Arango, D.C., Xiao, X., Brozik, S.M., Wang, J., Polsky, R., 2012. Multiplexed microneedle-based biosensor array for characterization of metabolic acidosis. Talanta 88, 739–742.
Mohan, A.V., Windmiller, J.R., Mishra, R.K., Wang, J., 2017. Continuous minimally-invasive alcohol monitoring using microneedle sensor arrays. Biosens. Bioelectron. 91, 574–579.
Nikolaus, N., Strehlitz, B., 2008. Amperometric lactate biosensors and their application in (sports) medicine, for life quality and wellbeing. Microchim. Acta 160 (1–2), 15–55.
Omole, O.O., Brocks, D.R., Nappert, G., Naylor, J.M., Zello, G.A., 1999. High-performance liquid chromatographic assay of (±)-lactic acid and its enantiomers in calf serum. J. Chromatogr. B: Biomed. Sci. Appl. 727 (1–2), 23–29.
Paliwal, S., Hwang, B.H., Tsai, K.Y., Mitragotri, S., 2013. Diagnostic opportunities based on skin biomarkers. Eur. J. Pharm. Sci. 50 (5), 546–556.
Petropoulos, K., Piermarini, S., Bernardini, S., Palleschi, G., Moscone, D., 2016. Development of a disposable biosensor for lactate monitoring in saliva. Sens. Actuators B: Chem. 237, 8–15.
Phypers, B., Pierce, J.M.T., 2006. Lactate physiology in health and disease. Contin. Educ. Anaesth. Crit. Care Pain 6 (3), 128–132.
Piano, M., Serban, S., Pittson, R., Drago, G., Hart, J.P., 2010. Amperometric lactate biosensor for flow injection analysis based on a screen-printed carbon electrode containing Meldola's Blue-Reinecke salt, coated with lactate dehydrogenase and NAD +. Talanta 82 (1), 34–37.
Rassaei, L., Olthuis, W., Tsujimura, S., Sudholter, E.J.R., van den Berg, A., 2014. Lactate biosensors: current status and outlook. Anal. Bioanal. Chem. 406 (1), 123–137.
Rathee, K., Dhull, V., Dhull, R., Singh, S., 2016. Biosensors based on electrochemical lactate detection: a comprehensive review. Biochem. Biophys. Rep. 5, 35–54.
Ren, J., Dean Sherry, A., Malloy, C.R., 2013. Noninvasive monitoring of lactate dynamics in human forearm muscle after exhaustive exercise by 1H-magnetic resonance spectroscopy at 7 T. Magn. Reson. Med. 70 (3), 610–619.
Rimachi, R., De Carvahlo, F.B., Orellano-Jimenez, C., Cotton, F., Vincent, J., De Backer, D., 2012. Lactate/pyruvate ratio as a marker of tissue hypoxia in circulatory and septic shock. Anaesth. Intensive Care 40 (3), 427–432.
Saito, N., Adachi, H., Tanaka, H., Nakata, S., Kawada, N., Oofusa, K., Yoshizato, K., 2017. Interstitial fluid flow-induced growth potential and hyaluronan synthesis of fibroblasts in a fibroblast-populated stretched collagen gel culture. Biochim. Biophys. Acta-Gen. Subj. 1861 (9), 2261–2273.
Sayeed, M., Murthy, P., 1981. Adenine nucleotide and lactate metabolism in the lung in endotoxin shock. Circ. Shock 8 (6), 657–666.
Sharma, S., Huang, Z., Rogers, M., Boutelle, M., Cass, A.E., 2016. Evaluation of a minimally invasive glucose biosensor for continuous tissue monitoring. Anal. Bioanal. Chem. 408 (29), 8427–8435.
Sharma, S., Saeed, A., Johnson, C., Gadegaard, N., Cass, A.E., 2017. Rapid, low cost prototyping of transdermal devices for personal healthcare monitoring. Sens. Bio-Sens. Res. 13, 104–108.
Shimomura, T., Sumiya, T., Ono, M., Ito, T., Hanaoka, T.-A., 2012. Amperometric l-lactate biosensor based on screen-printed carbon electrode containing cobalt phthalocyanine, coated with lactate oxidase-mesoporous silica conjugate layer. Anal. Chim. Acta 714, 114–120.
Shinbo, T., Sugiura, M., Kamo, N., 1979. Potentiometric enzyme electrode for lactate. Anal. Chem. 51 (1), 100–104.
Srivastava, S.K., Gupta, V.K., Dwivedi, M.K., Jain, S., 1995. Caesium PVC–crown (dibenzo-24-crown-8) based membrane sensor. Analytical Proceedings including Analytical Communications, pp. 21–23. Royal Society of Chemistry.
Srivastava, S.K., Gupta, V.K., Jain, S., 1996. PVC-based 2, 2, 2-cryptand sensor for zinc ions. Anal. Chem. 68 (7), 1272–1275.
Stanley, W.C., Gertz, E.W., Wisneski, J.A., Morris, D.L., Neese, R.A., Brooks, G.A., 1985. Systemic lactate kinetics during graded exercise in man. Am. J. Physiol.-Endocrinol. Metab. 249 (6), E595–E602.
Taurino, I., Sanzò, G., Antiochia, R., Tortolini, C., Mazzei, F., Favero, G., De Micheli, G., Carrara, S., 2016. Recent advances in third generation biosensors based on Au and Pt nanostructured electrodes. Trends Anal. Chem. 79, 151–159.
Thomas, N., Lähdesmäki, I., Parviz, B.A., 2012. A contact lens with an integrated lactate sensor. Sens. Actuators B: Chem. 162 (1), 128–134.
Umena, Y., Yorita, K., Matsuoka, T., Kita, A., Fukui, K., Morimoto, Y., 2006. The crystal structure of L-lactate oxidase from Aerococcus viridans at 2.1 Å resolution reveals the mechanism of strict substrate recognition. Biochem. Biophys. Res. Commun. 350 (2), 249–256.
Valdés-Ramírez, G., Li, Y.-C., Kim, J., Jia, W., Bandodkar, A.J., Nuñez-Flores, R., Miller, P.R., Wu, S.-Y., Narayan, R., Windmiller, J.R., 2014. Microneedle-based self-powered glucose sensor. Electrochem. Commun. 47, 58–62.
Valenza, F., Aletti, G., Fossali, T., Chevallard, G., Sacconi, F., Irace, M., Gattinoni, L., 2005. Lactate as a marker of energy failure in critically ill patients: hypothesis. Crit. Care 9 (6), 588–593.
Ventrelli, L., Marsilio Strambini, L., Barillaro, G., 2015. Microneedles for transdermal biosensing: current picture and future direction. Adv. Healthc. Mater. 4 (17), 2606–2640.
Vinod, K., 1995. Determination of lead using a poly (vinyl chloride)-based crown ether membrane. Analyst 120 (2), 495–498.
Windmiller, J.R., Zhou, N., Chuang, M.-C., Valdés-Ramírez, G., Santhosh, P., Miller, P.R., Narayan, R., Wang, J., 2011. Microneedle array-based carbon paste amperometric sensors and biosensors. Analyst 136 (9), 1846–1851.
Wu, F., Huang, Y., Huang, C., 2005. Chemiluminescence biosensor system for lactic acid using natural animal tissue as recognition element. Biosens. Bioelectron. 21 (3), 518–522.
Yola, M.L., Gupta, V.K., Eren, T., Şen, A.E., Atar, N., 2014. A novel electro analytical nanosensor based on graphene oxide/silver nanoparticles for simultaneous determination of quercetin and morin. Electrochim. Acta 120, 204–211.